27

DISINFECTANT AND BY-PRODUCT ANALYSIS IN WATER TREATMENT BY MEMBRANE INTRODUCTION MASS SPECTROMETRY

CHONGZHENG NA AND TERESE M. OLSON

Membrane introduction mass spectrometry (MIMS) is a state-of-the-art technique that combines the quick separation of volatile analytes from complex matrices using selective membranes with the precision offered by mass spectrometry (MS) on chemical identification and quantification [1]. Compared with gas or liquid chromatography (GC or LC) traditionally used in front of MS, the membrane separation technique has the advantages of being both simple, which minimizes sample preparation, and rapid, which makes real-time monitoring possible [2]. The use of a mass spectrometer as the detector also makes MIMS less subject to analytical interference, a frequent limitation of non-MS-based techniques such as calorimetry [3,4].

In comparison to the long history of MIMS development [5], its application to understanding drinking water disinfection has been a fairly recent endeavor (cf. Table 27.1). Disinfection is an important process in drinking water treatment that controls waterborne diseases by killing or inactivating pathogenic microorganisms such as bacteria, viruses, and protozoa [6]. In addition to inactivating pathogens, disinfectants can also react with trace-level organic matter, which is always present in water, to produce a variety of organic and inorganic disinfection by-products (DBPs), many of which have potential adverse, chronic health effects as a result of long-term exposure [7]. Understanding disinfectant speciation and DBP formation is an area of intensive research. Many common disinfectants and DBPs are either gaseous or volatile; therefore, they can be readily measured by MIMS.

Although MIMS has attracted much attention because of the aforementioned advantages over traditional analytical techniques for both disinfectants and DBPs [8], its use has so far been restricted to the cognoscenti of the research field. In this chapter, we present the protocols for implementing MIMS with the intention of expanding its access to a greater community of interested users. We focus our discussion on MIMS instruments using capillary membrane introduction probes [9], which have been the choice for water disinfection applications. More comprehensive reviews of MIMS development and applications are available in the literature [1,10].

27.1 METHODS

27.1.1 Capillary Membrane Introduction Probes

Capillary membrane introduction probes are typically configured with either a direct insertion membrane probe (DIMP) or an external one, as shown in Figure 27.1 [9]. DIMP must be designed and machined according to the configuration of the MS injection port. The basic idea is to place a piece of membrane tubing in close proximity to the ionization region of the mass spectrometer in order to enhance analyte permeation and improve response efficiency [11]. This can be achieved using two stainless steel tubes that have a slightly greater diameter than the inner diameter of the membrane tubing—one to direct the flow to the membrane tubing and the other to draw the flow back (cf. Figure 27.1A). Another advantage

Handbook of Mass Spectrometry, First Edition. Edited by Mike S. Lee.

TABLE 27.1 Disinfectants and Disinfection By-Products Analyzed by MIMS

Compound		Ionization	Mass Analyzer	Mass-to-Charge Ratio (m/z) Signature Peaks	Best Detection Limit (μM)[a]	References
Disinfectants	HOCl	EI	Quadrupole	[52]:[54] = 3:1	1.1[b]	Shang and Blatchley [3]
	Cl_2	EI	Quadrupole	[70]:[72]:[74] = 9:6:1		
	NH_2Cl	EI	Quadrupole	[51]:[53] = 3:3:1	1.1	Shang and Blatchley [3], Donnermair and Blatchley [26], Na and Olson [17], Lee et al. [4], Li and Blatchley [34], Yang et al. [35], Weaver et al. [36]
	$NHCl_2$	EI	Quadrupole	[49]:[50] = 3:1 [51]:[52] = 3:1 [85]:[87]:[89] = 9:6:1	0.28	
	NCl_3	EI	Quadrupole	[49]:[51] = 3:1 [84]:[86]:[88] = 9:6:1 [119]:[121]:[123] = 3:3:1	0.056	
Disinfection by-products	$CHCl_3$	EI	Quadrupole	[47]:[49] = 3:1 [48]:[50] = 3:1 [83]:[85]:[87] = 9:6:1	≤0.03	Shang et al. [37], Kristensen et al. [38], Weaver et al. [36]
	$CHBrCl_2$	EI	Quadrupole	[83]:[85]:[87] = 9:6:1 [127]:[129]:[131] = 3:4:1	≤0.0001	Kristensen et al. [38], Weaver et al. [36]
	$CHBr_2Cl$	EI	Quadrupole	[127]:[129]:[131] = 3:4:1	≤0.001	Weaver et al. [36]
	$CHBr_3$	EI	Quadrupole	[171]:[173]:[175] = 1:2:1	≤0.0003	Weaver et al. [36]
	$Cl_2CHC{\equiv}N$	EI	Quadrupole	[74]:[76] = 3:1 [82]:[84]:[86] = 9:6:1	≤0.005	Shang et al. [37], Li and Blatchley [34], Weaver et al. [36]
		CI	Quadrupole	[110]:[112]:[114] = 9:6:1	N/A	Shang et al. [37]
	$Cl_2N\text{-}CH_2\text{-}C{\equiv}N$	CI	Quadrupole	[89]:[91] = 3:1 [110]:[112]:[114] = 9:6:1 [125]:[127]:[129] = 9:6:1	≤0.2	Shang et al. [37]
	CNCl	EI	Quadrupole	[61]:[63] = 3:1	0.019	Shang et al. [37], Yang and Shang [39], Na and Olson [17] Li and Blatchley [34], Yang et al. [35]
		CI	Quadrupole	[62]:[64] = 3:1	N/A	Na and Olson [16]
		EI	Ion trap	[62]:[64] = 3:1	0.09	Na and Olson [16]
	CNBr	EI	Quadrupole	[^{79}Br]:[^{81}Br] = 1:1 [105]:[107] = 1:1	0.036	Yang and Shang [39], Weaver et al. [36]
	$Cl_2N\text{-}CH_3$	EI	Quadrupole	[98]:[100]:[102] = 9:6:1 [99]:[101]:[103] = 9:6:1	0.016	Li and Blatchley [34], Weaver et al. [36]
	$ClN{=}CH_2$	EI	Quadrupole	[63]:[65] = 3:1	N/A	Na and Olson [17]

[a] By convention, the concentrations of disinfectants are expressed in the equivalent milligram per liter as Cl_2: 1 mg/L Cl_2 = 1.4 μM.
[b] Total free chlorine measured after ammonification (i.e., adding ammonia to convert to both HOCl and Cl_2 into NH_2Cl).
CI, chemical ionization by methane; EI, electron impact; N/A, not available.

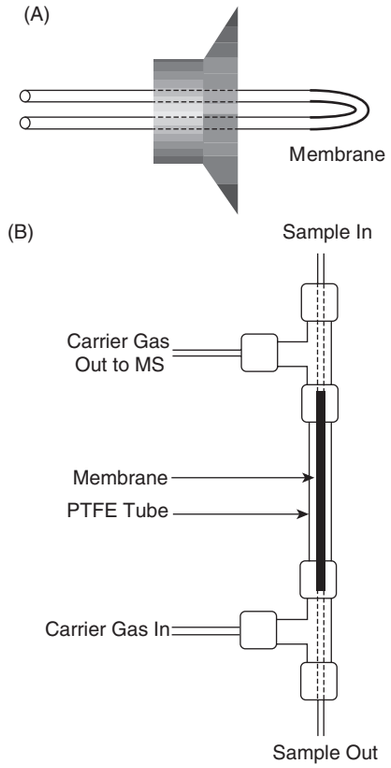

FIGURE 27.1 Membrane introduction probes using capillary membranes. (A) A direct inlet probe and (B) an external probe. Adapted from Riter et al. [9] with the permission of the American Chemical Society.

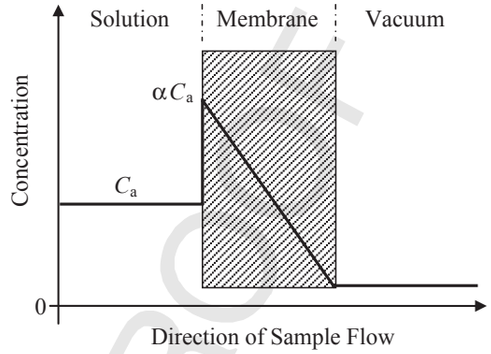

FIGURE 27.2 Conceptual model of the pervaporation through the MIMS membrane. C_a is the analyte concentration in the aqueous solution. α is the partitioning coefficient between the aqueous solution and the membrane. The linear concentration profile inside the membrane can be derived from steady-state conditions (see text for details). Adapted from Overney and Enke [15] with permission from the American Society of Mass Spectrometry.

of DIMP is that it does not require any carrier gas for operation. Thermocouples may be added outside the stainless steel tubes to preheat the solution and maximize performance.

By sacrificing some ionization efficiency, an external membrane introduction probe can be set up using an existing GC/MS system. A flow-through membrane cell can be set up as illustrated in Figure 27.1B and placed in the GC oven in place of the GC column. In the flow-through cell, the membrane tubing is placed in the center of a polytetrafluoroethylene (PTFE) tube having a greater diameter. The sample solution flows through the inner membrane tube, while a carrier gas such as helium flows between the two tubes. Volatile analytes permeate the membrane and are transferred to the mass spectrometer by the carrier gas.

The most common material used to make MIMS membranes is polydimethylsiloxane (PDMS), which is widely available from popular vendors. Because PDMS is hydrophobic, MIMS has the selectivity for molecules having high volatility (large Henry's constants) and high hydrophobicity (large octanol-water partition coefficients) [12]. Ideal analytes are compounds with water solubilities below 10,000 mg/L, vapor pressure in the range of 1000–2000 Pa, and log $K_{ow} = 2 - 3$ [13]. It has been noted that chlorination enhances a compound molecule's ability to pass through PDMS membranes; therefore, MIMS is particularly suitable for the studies of disinfectant chloramines and chlorinated DBPs [14]. Most of the PDMS tubings used in MIMS have an inner diameter of 0.64 mm, an outer diameter of 1.19 mm, and a length of a few centimeters.

27.1.2 Operational Principles

The processes through which an analyte passes through the MIMS membrane are collectively referred to as pervaporation. As shown in Figure 27.2, pervaporation includes three processes in which analyte molecules first partition between the aqueous phase and the membrane, then diffuse through the membrane, and eventually evaporate into the vacuum of the mass spectrometer [1,15]. The first process of partitioning is generally believed to be fast so that the concentrations of the analyte on the two sides of the solution–membrane interface are linearly related by a partitioning coefficient. The second process of diffusion is driven by the concentration gradient. The third process is generally the same for all analytes because the concentration on the vacuum side is essentially zero; therefore, according to the governing law of partitioning, the concentration on the membrane side is also zero. In summary, MIMS

is most sensitive for analyte molecules that have high rates of mass flow in pervaporation.

Once the analyte reaches the vacuum chamber of the mass spectrometer, they will be ionized and detected based on their mass-to-charge ratios (m/z). Although any ionization methods can be employed, current applications essentially use the standard electron impact (EI) method at 70 eV. However, because water can also pass through the membrane through evaporation, chemical ionization (CI) by H_3O^+ may also occur depending on the ionization environment inside the spectrometer. The ionization by H_3O^+ has been reported to occur for cyanogen chloride (CNCl) in a Saturn 4D ion-trap MS [16] but not in an Agilent 5972 quadrupole MS [17]. The CI in the ion trap MS may be represented by the following reactions:

$$H_2O + e \rightarrow H_2O^+ + 2e, \tag{27.1}$$

$$H_2O^+ + H_2O \rightarrow H_3O^+ + OH^-, \tag{27.2}$$

and

$$ClCN + H_3O^+ \rightarrow ClCNH^+ + OH. \tag{27.3}$$

The quantitative relation between solution concentration and MIMS response can be established by analyzing the mass transfer of the analyte through the semipermeable membrane. The mass transfer in the capillary probe membrane through pervaporation can be modeled as a hollow rod using Fick's law [18]:

$$\frac{1}{D_m}\frac{\partial C}{\partial t} = \frac{\partial^2 C}{\partial r^2} + \frac{1}{r}\frac{\partial C}{\partial r}, \tag{27.4}$$

where C is the concentration in the membrane, D_m is the diffusion coefficient in the membrane, t is the reaction time, and r is the radius from the center of tubular membrane. The boundary and initial conditions are

$$\text{BCs: } C(r = r_i, t) = \alpha C_a(t), \tag{27.5}$$

$$C(r = r_o, t) = 0, \tag{27.6}$$

$$\text{IC: } C(r, t \le t_d) = 0. \tag{27.7}$$

C_a is the bulk concentration in aqueous solution. α is the coefficient describing the partitioning of the analyte from the solution into the membrane. t_d is the delay time due to pump solution from the inlet to the membrane (as in direct inlet probes) or to carry the evaporated analyte to the mass spectrometer (as in external probes). r_i and r_o are inner and outer radii of the tubular membrane, respectively.

For the case when the aqueous concentration C_a is constant, such as when the MIMS is applied to analyze a standard solution or a nonreactive sample, Equations 27.4–27.7 have an analytical solution [19]:

$$C(r,t) = \alpha C_a \left[\frac{\ln(r_o/r)}{\ln(r_o/r_i)} + \pi \sum_{n=1}^{\infty} \frac{J_0(r_i\omega_n) J_0(r_o\omega_n) U_0(r\omega_n) e^{-D_m\omega_n^2 (t-t_d)}}{J_0^2(r_i\omega_n) - J_0^2(r_o\omega_n)} \right], \tag{27.8}$$

where $n = 1, 2, 3, \ldots$ (practically, $n = 5$ was used in calculation), J_0 = Bessel function of the first kind of zeroth order, $U_0(r\omega_n) = J_0(r\omega_n)Y_0(r_o\omega_n) - J_0(r_o\omega_n)Y_0(r\omega_n)$ with Y_0 = Bessel function of the second kind of zeroth order, and ω_n = the roots of $U_0(r_i\omega_n) = 0$. During analysis, the mass spectrometer detects the amount of analyte arriving at the vacuum chamber in each time interval τ, during which the mass spectrometer conducts a measurement. The MS intensity measurement, which responds to the rate of mass flow, can be calculated as follows:

$$I(t) = 2\pi r_o l \varphi \tau D_m \left.\frac{\partial C}{\partial r}\right|_{r=r_o}, \tag{27.9}$$

where l = length of the capillary membrane and φ = mass spectrometer multiplication factor. Combining Equations 27.8 and 27.9 gives the observed MIMS signal intensity:

$$I(t) = \frac{2\pi l \varphi \tau D_m \alpha C_a}{\ln(r_o/r_i)} \left[1 - r_o \ln(r_o/r_i) \pi \sum_{n=1}^{\infty} \frac{J_0(r_i\omega_n) J_0(r_o\omega_n) \frac{dU_0}{dr}(r_o\omega_n) e^{-D_m\omega_n^2 (t-t_d)}}{J_0^2(r_i\omega_n) - J_0^2(r_o\omega_n)} \right]. \tag{27.10}$$

These equations provide the basis for MIMS calibration and analysis of nonreacting analytes.

The calibration of MIMS requires a simple, preferably linear, relation between I and C_a. Such a relation can be derived by setting $t \rightarrow \infty$ in Equation 27.10 so that I approaches a steady-state value I_{ss} as follows:

$$I \rightarrow I_{SS} = \frac{2\pi l \varphi \tau D_m \alpha C_a}{\ln(r_o/r_i)} = \frac{C_a}{\sigma}. \tag{27.11}$$

This is a linear relation defined by a proportional factor $\sigma = \ln(r_o/r_i)/(2\pi/\varphi\tau D_m \alpha)$. In practice, one can pass a standard solution of known concentration through the membrane probe (i.e., known and constant C_a), wait long enough for the membrane to equilibrate (i.e., $t \to \infty$), and record the MIMS signal (i.e., $I \to I_{ss}$). Repetitions of this procedure will generate a set of C_a–I pairs. Linear regression using these data estimates σ, which we can now refer to as the calibration coefficient. Subsequently, we can use the MIMS to measure an unknown concentration and interpret it using σ.

When C_a is variable, such as when a reaction is in progress in the aqueous solution, Equations 27.4–27.7 must be solved numerically. To substitute the unknown partitioning constant α by the calibration coefficient σ, we can define a new membrane concentration variable:

$$C'(r,t) = \frac{C(r,t)}{\alpha\sigma}. \tag{27.12}$$

Replacing $C(r,t)$ with $C'(r,t)$ using Equation 27.9, Equations 27.1–27.4 become

$$\frac{1}{D_m}\frac{\partial C'}{\partial t} = \frac{\partial^2 C'}{\partial r^2} + \frac{1}{r}\frac{\partial C'}{\partial r}, \tag{27.13}$$

$$C'(r = r_i, t) = \frac{C_a(t)}{\sigma}, \tag{27.14}$$

$$C'(r = r_o, t) = 0, \tag{27.15}$$

and

$$C'(r, t \le t_d) = 0. \tag{27.16}$$

We should also rewrite Equation 27.9 according to Equations 27.13–27.16 to compute the MIMS response, as follows:

$$I(t) = -r_o \ln(r_o/r_i)\left.\frac{\partial C'}{\partial r}\right|_{r=r_o}. \tag{27.17}$$

With an initial guess of $C_a(t)$, $I(t)$ can be calculated by solving Equations 27.13–27.16 using fitting routines available in computer software packages such as Matlab [17].

27.1.3 MIMS Calibration and General Analysis

The concentrations of nonreactive analytes or analytes having half-lives greater than 30 min can be measured after MIMS is calibrated by a series of standard solutions with known concentrations. As indicated by Equation 27.11, given enough time for the instrument to respond (typically a few minutes), a linear relationship can be obtained between MS ion counts and analyte concentration. An example is shown in Figure 27.3 for cyanogen chloride (CNCl), a gaseous and toxic DBP [17]. Similar relationships between I_{ss} and C_a have been observed for chloramines and other DBPs (cf. Table 27.1). For the example shown in Figure 27.3, a linear regression gives $\sigma = 1.59(\pm 0.01) \times 10^{-8}$ M/(ion count). From a sensitivity perspective, a small calibration coefficient is desirable.

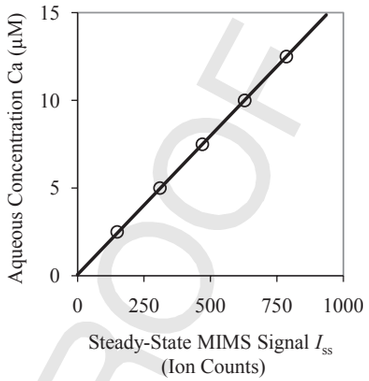

FIGURE 27.3 A typical calibration curve for cyanogen chloride (CNCl) at pH 7.0 (±0.1) and 25°C. Experimental data are represented by gray circles, and the black line is the linear fit with Equation 27.8. Adapted from Na and Olson [17] with the permission of the American Chemical Society.

The sensitivity of MIMS can be improved by elevating the temperature of the sample solution and that of the membrane to 60–70°C, provided that the analyte is stable at elevated temperatures. The reason for the improved sensitivity is that the elevation of temperature increases both the permeability and the diffusivity of the analyte through the membrane. However, further increase of temperature will decrease MIMS sensitivity due to the increase of the permeability of water near its boiling point, which interferes with the analyte for permeation through the membrane [3]. Other operational parameters such as liquid and airflow rates generally have little effect on the performance of MIMS.

An important question regarding calibration is whether σ remains constant and whether the MIMS needs to be recalibrated under varying solution

chemistry, such as pH and ionic strength. To our knowledge, there is no systematic study that has been performed on the effects of ionic strength. Shang and Blatchley [3] have recommended that for chloramines, MIMS should be calibrated for the conditions under which measurements will be made. In our own experiments, we observed that for CNCl, σ varied between $1.16(\pm 0.01) \times 10^{-8}$ and $2.10(\pm 0.01) \times 10^{-8}$ M/(ion count) from pH 4 to 8 although the variation was not systematic. In summary, we recommend that MIMS should be calibrated for the conditions of measurement until the effects of solution chemistry are proven to be negligible.

27.1.4 MIMS Analysis of Analytes Under Reaction

For analytes having half-lives shorter than 30 min in the sample solution, the delay of MIMS response due to mass transfer must be accounted for to convert MS ion counts to concentration. This is particularly important for measuring disinfectant or DBF concentrations because unless disinfectants are quenched, there is almost certain to be reactions between disinfectants and natural organic matter (NOM) always present in natural water (i.e., DBP formation) [20] or reactions between disinfectants and DBPs (i.e., DBP decay). Another situation requiring consideration of MIMS response times is when relatively fast reaction kinetics is of interest [17].

As indicated by Equations 27.12–27.16, the conversion of $I(t)$ to $C_a(t)$ requires the knowledge of D_m and t_d, in addition to that of σ, to solve the equations numerically by iteration. According to our previous experience with CNCl, D_m and t_d can be estimated from the time-resolved MIMS responses of standard solutions. As shown in Figure 27.4, a typical time-resolved MIMS response curve consists of three segments. First, there is a delay of less than 1 min due to pumping the solution from the probe inlet to the membrane tubing. Second, there is another delay segment of ca. 2 min due to the diffusion in the membrane. Finally, the MIMS response reaches its steady-state value of ion counts. By fitting the calibration measurements to Equation 27.10, D_m and t_d can be estimated. For the example shown in Figure 27.4, we have $D_m = 3.5(\pm 0.1) \times 10^{-6}$ cm^2/s and $t_d = 0.48(\pm 0.01)$ min by least-square nonlinear regression.

With the estimates of D_m, t_d, and σ and an initial guess of $C_a(t)_{guess}$, $I^*(t)$ can be calculated by solving Equations 27.13–27.17. The calculated profile, $I^*(t)$, is then compared with the experimental intensity measurements, and the difference between $I^*(t)$ and $I(t)$ are used to adjust $C_a(t)$. $I^*(t)$ is then recalculated and the process is reiterated until the difference between $I^*(t)$ and $I(t)$ becomes negligible. Upon minimizing the difference, an estimate

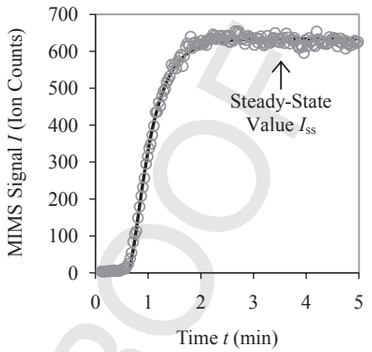

FIGURE 27.4 A time-resolved MIMS measurement of 10 μM CNCl standard at pH 7.0 and 25°C. Experimental data are represented by gray circles, and the black line is the nonlinear fit with Equation 27.7. I_{ss} is the steady-state MIMS signal. Adapted from Na and Olson [17] with the permission of the American Chemical Society.

of the aqueous concentration $C_a(t)$ is obtained. The final nth estimate, $C_a(t)n$, is assumed to be equal to the actual aqueous concentration $C_a(t)$. It may be necessary to filter high-frequency noise from the $I(t)$ data set to avoid long computation times. To expedite the transformation, for example, $I(t)$ can first be represented by a polynomial function $I_{fit}(t)$, in which the polynomial coefficients are fit with a nonlinear regression routine [17].

In summary, the procedure to estimating $C_a(t)$, from the experimental measurement $I(t)$, involves the following steps:

1. Estimate D_m, t_d, and σ using standard solutions with known concentrations of the analyte.
2. Fit the raw MIMS data $I(t)$ to a polynomial function, $I_{fit}(t)$.
3. Establish an initial guess for $C_a(t)$ as $C_a(t)_{guess} = \sigma I_{fit}(t)$.
4. Numerically solve Equations 27.13–27.16 using $C_a(t)_{guess}$ together with D_m, t_d, and σ. A prediction for $I_{fit}(t)$, $I_{fit}{}^*(t)$, is calculated based on Equation 27.17.
5. A nonlinear regression routine is applied to iteratively adjust the polynomial coefficients of $C_a(t)_{guess}$ and minimize the difference between $I_{fit}(t)$ and $I_{fit}{}^*(t)$. The explained sum of squares (ESS) should be calculated as

$$\text{ESS} = \sum [I_{fit}(t) - I_{fit}{}^*(t)]^2. \qquad (27.18)$$

The final result $C_a(t)$ was obtained by minimizing ESS.

An example of the fitting routine written in Matlab can be found in the supporting information of Na and Olson [17]. The robustness of the entire procedure should be evaluated to ensure the representativeness of the numerical solution by performing the iteration with different $C_a(t)_{guess}$ values.

27.2 APPLICATIONS

MIMS has been applied to analyzing disinfectants and DBPs in three different ways. The applications of MIMS include (1) understanding the speciation of chlorine-based disinfectants, (2) identifying and quantifying DBPs, and (3) elucidating the mechanisms of DBP formation and stability through kinetic measurements. The first two applications can be performed following the procedures outlined in Section 27.2.3. The third application may involve the employment of the protocols outlined in Section 27.2.4.

27.2.1 Speciation of Chlorine-Based Disinfectants

Free chlorine and inorganic chloramines are the main disinfectants used by most public drinking water treatment facilities in the United States [21–23]. The chemical species of free chlorine are dissolved chlorine gas (Cl_2), hypochlorous acid (HOCl), and its conjugate base hypochlorite (OCl^-) [24]. Inorganic chloramines are formed by the reactions of ammonia (sometimes added intentionally) and nitrogenous organic matter. The chloramine species include monochloramine (NH_2Cl), dichloramine ($NHCl_2$), and trichloramine (NCl_3) with monochloramine being the main, desirable species in water treatment. The transformation between free chlorine and chloramines is quite complicated, especially in the presence of common constituents of natural water such as carbonate, bromide, nitrite, and NOM [25].

The greatest incentive for using MIMS over traditional colorimetry is that the traditional method cannot distinguish inorganic chloramines from organic ones that have poor disinfection efficiency against pathogenic microorganisms in drinking water and wastewater [3,4,26]. In swimming pools, chloramines, in particular di- and trichloramines, are the sources of offensive chlorine odor and irritation to swimmers' eyes.

In principle, all of the aforementioned species may be measured by MIMS. As shown in Figure 27.5 [3], gaseous Cl_2, HOCl, NH_2Cl, $NHCl_2$, and NCl_3 can be measured directly with distinctive *m/z* signatures on MIMS spectra. The relative abundances of the signature peaks, as analyzed in Table 27.1, obey the isotopic ratios of $[^{35}Cl]:[^{37}Cl] \approx 3:1$ [27]. The OCl^- concentration may be computed from that of HOCl and pH:HOCl $H^+ + OCl^-$ ($pK_a = 7.55$ at 25°C) [24].

In practice, the direct measurement of free chlorine using the MIMS peaks of Cl_2 or HOCl is constrained by their high detection limits. Note that a chlorine standard having a concentration 100 times greater than that of the monochloramine standard has to be used to generate a similar response (i.e., Figure 27.5A vs. B). In comparison, direct MIMS measurements of mono-, di-, and trichloroamines in drinking water are achievable due to their low detection limits, which are approximately 1.1, 0.28, and 0.056 μM, respectively [3,4]. The disinfectant concentration in drinking water often exceeds 2.8 μM (0.2 mg/L as Cl_2) [6].

To circumvent the high detection limit of free chlorine, ammoniation can be performed before MIMS measurement. Ammoniation converts free chlorine to monochloramine by adding excess amount of ammonia (NH_3; in the form of ammonium chloride, NH_4Cl) [3]. The difference of monochloramine before and after ammoniation gives the concentration of free chlorine.

The standard solutions used to calibrate MIMS can be readily prepared according to well-established methods. Free chlorine can be purchased in the form of sodium hypochlorite (NaOCl) solution. It can be standardized by either the UV absorbance of OCl^- at 292 nm ($\varepsilon_{OCl,max} = 350$ M/cm, 25°C and pH > 9.5) [24,28,29] or standard diethyl-*p*-phenylenediamine (DPD) titration [30]. Standards containing monochloramine and dichloramine can be prepared by slowly pouring a free chlorine solution over an ammonium chloride solution at a chlorine-to-ammonia molar ratio of 1.31:1.00 under rapid stirring. One should wait for 1 h for the reactions to complete in darkness [3]. Standards of trichloramine can be prepared similarly but at a chlorine-to-ammonia molar ratio of 3.15:1.00. The pH of the standard solution can be adjusted to that of the sample solution by phosphate buffers. The standard solutions can be standardized by DPD titration [30].

27.2.2 Identification and Quantification of DBPs

The application of MIMS to the measurement of DBPs in swimming pools has recently attracted considerable attention. Because of the typical high organic load found in swimming pools from sunscreens, perspiration, urine, and other sources, the chlorination of pool water often generates high concentrations of DBPs [31]. The volatile DBPs are particularly troublesome because they can be taken up by swimmers through respiration and skin absorption [32]. The high DBP concentrations in swimming pools are likely to be well above MIMS detection limits, unlike drinking water applications where much lower concentrations are typical (cf. Table 27.1).

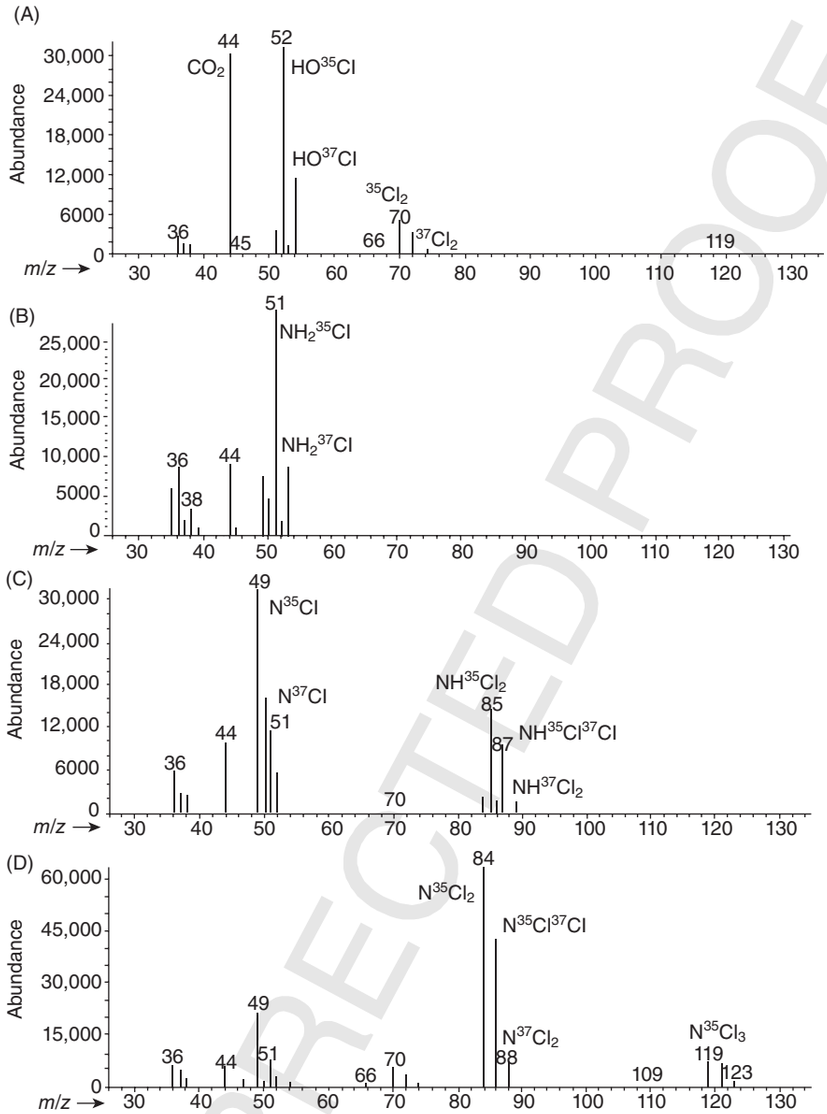

FIGURE 27.5 Representative EI mass spectra ($35 \leq m/z \leq 125$) of (A) free chlorine (2000 mg/L as Cl_2), (B) monochloramine (40 mg/L as Cl_2), (C) dichloramine (20 mg/L as Cl_2), and (D) trichloramine (20 mg/L as Cl_2). Reprinted from Shang and Blatchley [3] with the permission of the American Chemical Society.

The identification of DBPs can be challenging because the volatile compounds form a mixture after they pass the semipermeable silicone membrane in MIMS. The challenge is somewhat alleviated for halogenated DBPs by the isotopic signatures of chlorine and bromine. The halogenated compounds that have been identified as DBPs in the literature are summarized in Table 27.1. They include several trihalomethanes (THMs) such as chloroform ($CHCl_3$), dichlorobromomethane ($CHBrCl_2$), dibromochloromethane ($CHBr_2Cl$), and bromoform ($CHBr_3$). Other DBPs are dichloroacetonitrile ($Cl_2CHC{\equiv}N$), *N*,*N*-dichloroaminoacetonitrile ($Cl_2N{-}CH_2C{\equiv}N$), cyanogen chloride (CNCl), cyanogen bromide (CNBr), and dichloromethylamine (CH_3NCl_2). Like chloramines, their signature *m/z* peaks also obey the isotopic ratios of $[^{35}Cl]:[^{37}Cl] \approx 3{:}1$ and $[^{79}Br]:[^{81}Br] \approx 1{:}1$. The distinctive MIMS peaks of volatile disinfection products are summarized in Table 27.1.

Even for chlorinated compounds, their *m/z* signatures can still overlap when more than one of them is

present in a sample. This is particularly problematic in quantification. For example, $CHBr_2Cl$ has the most abundant response at *m/z* 127. However, $CHBrCl_2$ can also contribute to this peak. When both of them are present, the contribution from $CHBrCl_2$ has to be subtracted from the total abundance at *m/z* 127:

$$I_{m/z\ 127}(CH^{79}Br^{35}Cl^{\bullet+}\ \text{from}\ CHBrCl_2) = I_{m/z\ 127}(\text{total}) - I_{m/z\ 127}(CH^{79}Br^{35}Cl^{\bullet+} + \text{from}\ CHBr_2Cl), \quad (27.19)$$

$$I_{m/z\ 127}(CH^{79}Br^{35}Cl^{\bullet+} + \text{from}\ CHBr_2Cl) = \chi I_{m/z\ 83}(CH^{35}Cl^{35}Cl^{\bullet+} + \text{from}\ CHBrCl_2), \quad (27.20)$$

where χ is the abundance ratio of the peaks at *m/z* 127 and 83 measured with $CHBr_2Cl$ standards. According to Table 27.1, $CHCl_3$ can also contribute to *m/z* 83. If $CHCl_3$ is in solution, then its contribution must also be considered:

$$I_{m/z\ 83}(CH^{35}Cl^{35}Cl^{\bullet+} + \text{from}\ CHBrCl_2) = I_{m/z\ 83}(\text{total}) - I_{m/z\ 83}(CH^{35}Cl^{35}Cl^{\bullet+} + \text{from}\ CHCl_3). \quad (27.21)$$

With the addition of even more volatile components in a water sample, the deconvolution of their contributions to specific MIMS peaks can quickly become unmanageable. The application of tandem mass spectrometry (MS/MS) can be helpful for cases where two different fragments from two different sources give the same *m/z* value within uncertainty. Like the case mentioned above, MS/MS cannot distinguish the sources by further fragmenting the ions because different sources give the same ion at the specified *m/z*. One possible solution to such a problem may be to place a short GC column between the semipermeable membrane and the MS ionization chamber, which can be readily envisioned for the external MIMS configuration. We are, however, not aware of any study that has incorporated chromatography into MIMS. Nevertheless, the complexity of the volatile composition of a sample should be checked on before MIMS is considered.

Another advantage of MIMS is that it does not require sample preparation and can be operated in a flow-through mode; therefore, MIMS can be employed for automatic, on-line monitoring. A recent study that continuously monitored THMs in a Danish pool has shown that the evaporation of volatile DBPs was greatly enhanced by the activities of the swimmers when the pool was open [2]. Such long-term monitoring data are expected to provide valuable insights for improving the management of water treatment in swimming pools so that the adverse health effects of swimming in chlorinated pools can be minimized.

27.2.3 Formation and Stability of DBPs

MIMS has been shown to be suitable for studying the kinetics of DBP formation and decay reactions that have half-lives greater than the mass-transfer delay (typically a few minutes) [16,17]. A traditional technique for studying disinfection reactions is UV-vis spectrophotometry [33]; however, not all reactants and products have significant light absorption. Another option to study kinetics besides direct measurement is quenching the reaction; however, this method only works when the reaction can be stopped by either a rapid change in the experimental condition or the addition of chemicals to exhaust a reactant. Compared with spectrophotometry and quenching, MIMS has the advantage of being applicable to most volatile compounds and requiring minimum sample preparation.

To perform kinetic studies in the laboratory, the MIMS should be connected with a reactor and set up in a continuous flow-through mode (i.e., in-line MIMS). An example of such a configuration is shown in Figure 27.6 [16]. Because the analytes are volatile, void space should be minimized in the setup. One strategy, as illustrated in Figure 27.6, is to direct the solution back to the reactor after MIMS measurement. If this strategy is used, the reactor volume should be large enough to ensure that the loss of volatile components in the MIMS will not affect reaction progress.

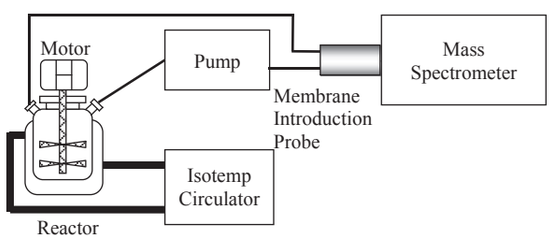

FIGURE 27.6 An example of in-line MIMS system used in kinetic studies. This system consists of a constant temperature and well-mixed batch reactor, a high performance liquid chromatography (HPLC) piston pump (Acuflow Series I, Lab Alliance Inc., State College, PA), a direct membrane inlet probe (MIMS Technology), and a Saturn 4D ion trap (Varian) or Hewlett-Packet 5972 quadrupole mass spectrometer (MS) (Agilent Technologies, Santa Clara, CA). The MS operated in the electron impact (EI) mode. Reprinted from Na and Olson [16] with the permission of the American Chemical Society.

Depending on the half-life of the reaction, one may decide whether the mass-transfer delay should be included in data analysis. For the MIMS system that has generated the CNCl spectrum in Figure 27.4, the total delay is approximately 2 min. If a 5% measurement discrepancy is assumed to occur in this period, then a pseudo-first-order reaction with a half-life greater than 27 min would not require consideration of the delay (i.e., $t_{1/2} \geq 2$ min $\times$ [ln(0.5)/ln(0.95)]). This is the case for CNCl decay in the presence of free chlorine, which has a half-life of ca. 60 min [16].

The kinetic data must be analyzed following the procedure outlined in Section 27.2.4 for reactions with a half-life close to or shorter than ca. 30 min. This is the case for the formation of CNCl from the chlorination of glycine, a prevalent nitrogenous compound in natural water [17]. Extensive calibration is required to obtain important parameters such as D_m, t_d, and σ.

Because a mass spectrometer is a universal detector, MIMS offers the advantage that unexpected, short-lived reaction intermediates can often be spectrally identified during kinetic studies. *N*-chloromethylimine ($ClN{=}CH_2$) is such an example intermediate that was found to play an important role in the formation of the DBP CNCl due to the reaction of chlorine and glycine [17] (cf. Table 27.1). The direct observation and identification of $ClN{=}CH_2$ by MIMS greatly simplified the process of elucidating the reaction pathway for CNCl formation.

REFERENCES

1. Johnson, R.C., Cooks, R.G., Allen, T.M., Cisper, M.E., Hemberger, P.H. (2000) Membrane introduction mass spectrometry: trends and applications. *Mass Spectrometry Reviews*, *19*, 1–37.
2. Kristensen, G.H., Klausen, M.M., Hansen, V.A., Lauritsen, F.R. (2010) On-line monitoring of the dynamics of trihalomethane concentrations in a warm public swimming pool using an unsupervised membrane inlet mass spectrometry system with off-site real-time surveillance. *Rapid Communications in Mass Spectrometry*, *24*, 30–34.
3. Shang, C., Blatchley, E.R. (1999) Differentiation and quatification of free chlorine and inorganic chloramines in aqueous solution by MIMS. *Environmental Science & Technology*, *33*, 2218–2223.
4. Lee, W., Westerhoff, P., Yang, X., Shang, C. (2007) Comparison of colorimetric and membrane introduction mass spectrometry techniques for chloramine analysis. *Water Research*, *41*, 3097–3102.
5. Hoch, G., Kok, B. (1963) A mass spectrometer inlet system for sampling gases dissolved in liquid phases. *Archives of Biochemistry and Biophysics*, *101*, 160–170.
6. Haas, C.N. (1999) Disinfection. In *Water Quality and Treatment*, edited by Letterman, R.D. New York: McGraw Hill.
7. USEPA. (2003) National primary drinking water standards. EPA *816-F-03-016*.
8. Richardson, S.D. (2008) Environmental mass spectrometry: emerging contaminants and current issues. *Analytical Chemistry*, *80*, 4373–4402.
9. Riter, L.S., Peng, Y.A., Noll, R.J., Patterson, G.E., Aggerholm, T., Cooks, R.G. (2002) Analytical performance of a miniature cylindrical ion trap mass spectrometer. *Analytical Chemistry*, *74*, 6154–6162.
10. Ketola, R.A., Kotiaho, T., Cisper, M.E., Allen, T.M. (2002) Environmental applications of membrane introduction mass spectrometry. *Journal of Mass Spectrometry*, *37*, 457–476.
11. Bier, M.E., Cooks, R.G. (1987) Membrane interface for selective introduction of volatile compounds directly into the ionization chamber of a mass spectrometer. *Analytical Chemistry*, *59*, 597–601.
12. Kotiaho, T., Lauritsen, F.R., Choudhury, T.K., Cooks, R.G., Tsao, G.T. (1991) Membrane introduction mass-spectrometry. *Analytical Chemistry*, *63*, 1794–1801.
13. Lopez-Avila, V., Benedicto, J., Prest, H., Bauer, S. (1999) Automated MIMS for direct analysis of organic compounds in water. *American Laboratory*, *31*, 32.
14. Geinoz, S., Rey, S., Boss, G., Bunge, A.L., Guy, R.H., Carrupt, P.A., Reist, M., Testa, B. (2002) Quantitative structure-permeation relationships for solute transport across silicone membranes. *Pharmaceutical Research*, *19*, 1622–1629.
15. Overney, F.L., Enke, C.G. (1996) A mathematical study of sample modulation at a membrane inlet mass spectrometer—potential application in analysis of mixtures. *Journal of the American Society for Mass Spectrometry*, *7*, 93–100.
16. Na, C., Olson, T.M. (2004) Stability of cyanogen chloride in the presence of free chlorine and monochloramine. *Environmental Science & Technology*, *38*, 6037–6043.
17. Na, C., Olson, T.M. (2006) Formation of cyanogen chloride from glycine in chlorination. *Environmental Science & Technology*, *40*, 1469–1477.
18. Sysoev, A.A., Ketola, R.A., Mattila, I., Tarkiainen, V., Kotiaho, T. (2001) Application of the numerical model describing analyte permeation through hollow fiber membranes into vacuum for determination of permeation parameters of organic compounds in a silicone membrane. *International Journal of Mass Spectrometry*, *212*, 205–217.
19. Jaeger, J.C. (1940) Radial heat flow in circular cylinders with a general boundary condition. *Journal and Proceedings of Royal Society of New South Wales*, *74*, 342–352.
20. Westerhoff, P., Mash, H. (2002) Dissolved organic nitrogen in drinking water supplies: a review. *Journal of Water Supply Research and Technology-Aqua*, *51*, 415–448.
21. Connell, G.F., Routt, J.C., Macler, B., Andrews, R.C., Chen, J.M., Chowdhury, Z.K., Crozes, G.F., Finch, G.B., Hoehn, R.C., Jacangelo, J.G., Penkal, A., Schaeffer, G.R., Schulz, C.R., Uza, M.P. (2000) Committee report: disinfection at

large and medium-size systems. *Journal American Water Works Association*, *92*, 32–43.

22. Connell, G.F., Routt, J.C., Macler, B., Andrews, R.C., Chen, J.M., Chowdhury, Z.K., Crozes, G.F., Finch, G.B., Hoehn, R.C., Jacangelo, J.G., Penkal, A., Schaeffer, G.R., Schulz, C.R., Uza, M.P. (2000) Committee report: disinfection at small systems. *Journal American Water Works Association*, *92*, 24–31.
23. Haas, C.N., Jacangelo, J.G., Bishop, M.M., Cameron, C.D., Chowdhury, Z.K., Connell, G.F., Doty, G.A., Finch, G.R., Gates, D.J., Greenberg, A.E., Hoehn, R.C., Huebner, W.B., Jensen, J.N., Lange, A.L., Long, B.W., Moyer, N.P., Nagel, W.H., Noran, P.F., Palin, A.T., Regli, S.E., Routt, J.C., Symons, J.M., Thompson, C.K., Voyles, C.F. (1992) Survey of water utility disinfection practices. *Journal American Water Works Association*, *84*, 121–128.
24. Morris, J.C. (1966) Acid ionization constant of HoCl from 5 to 35 degrees. *Journal of Physical Chemistry*, *70*, 3798–3805.
25. Vikesland, P.J., Ozekin, K., Valentine, R.L. (2001) Monochloramine decay in model and distribution system waters. *Water Research*, *35*, 1766–1776.
26. Donnermair, M.M., Blatchley, E.R. (2003) Disinfection efficacy of organic chloramines. *Water Research*, *37*, 1557–1570.
27. McLafferty, F.W., Turecek, F. (1993) *Interpretation of Mass Spectra*, 4th ed. Sausalito, CA: University Science Books.
28. Galal-Gorchev, H., Morris, J.C. (1965) Formation and stability of bromamide bromimide and nitrogen tribromide in aqueous solution. *Inorganic Chemistry*, *4*, 899–905.
29. Friedman, H.L. (1953) On the ultraviolet absorption spectra of uninegative ions. *Journal of Chemical Physics*, *21*, 318–322.
30. American Public Health Association, American Water Works Association, Water Pollution Control Federation, and Water Environment Federation. (1995) *Standard Methods for the Examination of Water and Wastewater*, 19th ed., Vol. (4500-Cl F and G for free chlorine, 4500-CN-D for KCN, and 4500-CN-J for CNCl). New York [etc.]: American Public Health Association.
31. Zwiener, C., Richardson, S.D., De Marini, D.M., Grummt, T., Glauner, T., Frimmel, F.H. (2007) Drowning in disinfection byproducts? Assessing swimming pool water. *Environmental Science & Technology*, *41*, 363–372.
32. Weisel, C.P., Richardson, S.D., Nemery, B., Aggazzotti, G., Baraldi, E., Blatchley, E.R., Blount, B.C., Carlsen, K.H., Eggleston, P.A., Frimmel, F.H., Goodman, M., Gordon, G., Grinshpun, S.A., Heederik, D., Kogevinas, M., LaKind, J.S., Nieuwenhuijsen, M.J., Piper, F.C., Sattar, S.A. (2009) Childhood asthma and environmental exposures at swimming pools: state of the science and research recommendations. *Environmental Health Perspectives*, *117*, 500–507.
33. Margerum, D.W., Gray, E.T., Huffman, R.P. (1978) Chlorination and the formation of N-Chloro compounds in water treatment. In *Organometals and Organometalloids. ACS Symposium Series*, *82*, 278–291.
34. Li, J., Blatchley, E.R. (2007). Volatile disinfection byproduct formation resulting from chlorination of organic-nitrogen precursors in swimming pools. *Environmental Science & Technology*, *41*, 6732–6739.
35. Yang, X., Shang, C., Westerhoff, P. (2007) Factors affecting formation of haloacetonitriles, haloketones, chloropicrin and cyanogen halides during chloramination. *Water Research*, *41*, 1193–1200.
36. Weaver, W.A., Li, J., Wen, Y.L., Johnston, J., Blatchley, M.R., Blatchley, E.R. (2009) Volatile disinfection byproduct analysis from chlorinated indoor swimming pools. *Water Research*, *43*(13), 3308–3318.
37. Shang, C., Gong, W.L., Blatchley, E.R. (2000) Breakpoint chemistry and volatile byproduct formation resulting from chlorination of model organic-N compounds. *Environmental Science & Technology*, *34*(9), 1721–1728.
38. Kristensen, G.H., Klausen, M.M., Hansen, V.A., Lauritsen, F.R. (2010) On-line monitoring of the dynamics of trihalomethane concentrations in a warm public swimming pool using an unsupervised membrane inlet mass spectrometry system with off-site real-time surveillance. *Rapid Communications in Mass Spectrometry*, *24*(1), 30–34.
39. Yang, X., Shang, C. (2005) Quantification of aqueous cyanogen chloride and cyanogen bromide in environmental samples by MIMS. *Water Research*, *39*(9), 1709–1718.

To